ATATÜRK ÜNİVERSİTESİ YAYINLARI
ATATURK UNIVERSITY PUBLICATIONS

Research Article DOI: 10.5281/zenodo.14533858

Impact of soaking duration on chitosan yield and functional properties from shrimp shell

Siti Asma Che AZIZ [1]
[1] Centre for Telecommunication Research and Innovation (CeTRI), Faculty of Electronics and Computer Technology and Engineering, Universiti Teknikal Malaysia Melaka, Malaysia

Siti Amaniah Mohd CHACHULI [1]
[1] Centre for Telecommunication Research and Innovation (CeTRI), Faculty of Electronics and Computer Technology and Engineering, Universiti Teknikal Malaysia Melaka, Malaysia

Nur Hazahsha SHAMSUDIN [2]
[2] Department of Engineering, Faculty of Technology and Electrical Engineering, Universiti Teknikal Malaysia Melaka, Malaysia

ABSTRACT

This study investigates the effect of varying soaking times on the production of chitosan from shrimp shells. A sample of fresh shrimp shells was obtained from a market in Malacca, Malaysia, and pre-treated by washing, drying, and pulverizing into a homogeneous powder. The synthesis process involved three primary steps: demineralization, deproteinization, and deacetylation. Each step was executed under different conditions for four samples (S1-S4) to examine the impact of soaking duration on chitosan yield and properties. Demineralization was achieved using 1 M HCl, while deproteinization involved treatment with 1 M NaOH, both with varying soaking times. Deacetylation was conducted with 12.5 M NaOH at different temperatures and durations. The resultant chitosan was characterized using Fourier Transform Infrared (FTIR) spectroscopy, X-ray diffraction (XRD), and UV-Vis spectroscopy. The FTIR spectra confirmed the presence of characteristic chitosan functional groups, with higher degrees of deacetylation (DD%) corresponding to increased soaking times. XRD analysis indicated an amorphous structure for all samples, with S4 displaying the lowest crystallinity at the highest DD%. UV-Vis analysis confirmed that all samples were soluble in 1% acetic acid, suggesting good purity. The findings demonstrate that while soaking times affect the DD% and crystallinity of chitosan, all samples remained soluble and suitable for further applications. This work demonstrates that while soaking times affect the DD% and crystallinity of chitosan, all samples remained soluble and suitable for further applications. This study provides insights into optimizing chitosan production with variations in soaking time conditions.

Keywords: Chitin, Chitosan, Soaking Time

INTRODUCTION

Chitin and chitosan are both non-toxic, biocompatible, and biodegradable biopolymers. Additionally, they act as antimicrobial and hydrating agents. They are the second-most abundant natural polysaccharides on the planet after cellulose and are derived from the exoskeletons of marine crustaceans such as crabs [1], lobsters [2], shrimp [3], and squid pens [4]. Different sources of crustacean shell waste result in different chitin content. For example, black tiger shrimp (Penaeus monodon) waste has the highest chitin content [5]. Chitosan is a chitin derivative. In contrast to chitin, chitosan is soluble in a wide variety of solvents, particularly acidic aqueous solvents, which enables it to act as a cationic polyelectrolyte. In recent years, chitosan has surpassed chitin as the preferred material due to its greater tractability during the solution process. Chitosan's applications have been discussed previously [6] and include cosmetics, water engineering, paper manufacturing, textile manufacturing, food processing, agriculture, photography, and biomedical applications.

There are many literature studies on the preparation of chitin and chitosan from marine sources. However, two common methods used are the chemical method [6] and the biological method [7,8]. The chemical method involves three different steps: demineralization, deproteinization and deacetylation. The demineralization step is used to remove the calcium carbonate ($CaCO_3$) in the shell by agitation using different hydrochloric acid (HCl) concentrations. Traditionally, the process of deproteinization involved using aqueous solutions of sodium hydroxide (NaOH) or potassium hydroxide (KOH). The effectiveness of the deproteinization process depends on the temperature, concentration and ratio of its solution/solvent[5]. Essentially, in the deproteinization process an alkaline solution is used to hydrolyze the covalent bonds between the chitin and protein. The end product of this step will produce chitin [9]. Deacetylation reactions have also been observed as an adverse reaction during the demineralization process with high acid concentrations. According to [9], to overcome this problem, mild acid was preferred for use in the demineralization process. During demineralization, the conditions in terms of pH, time, and temperature will affect the molecular weight [10]. A high degree of acetylation was obtained by [10] using 0.25 M HCl at room temperature within 15 min.

The objective of this study was to investigate the effect of varying soaking times on the synthesis and characterization of chitosan derived from shrimp shells. By modifying the soaking times during the deproteinization and deacetylation stages, the study aims to understand how these changes influence key properties such as the degree of deacetylation (DD%), crystallinity, and solubility of the resulting chitosan. The study also employs techniques such as FTIR and XRD to analyze the functional groups

Received 04.09.2024
Revised 12.11.2024
Accepted 29.11.2024
Publication Date 20.12.2024

Corresponding author:
Siti Asma Che AZIZ
E-mail:
sitiasma@utem.edu.my

Cite this article: Aziz S. A. C., Chachuli A. A. M., Shamsudin N. H. Impact of Soaking Duration on Chitosan Yield and Functional Properties from Shrimp Shell. *NanoEra*. 2024;4(2):53-59

and structural characteristics of chitosan under different processing conditions. This investigation will provide insights into optimizing chitosan production for various industrial and biomedical applications.

MERHOD

Pre-treated Sample

The 1.5 kg sample of fresh shrimp shells was taken from a market in Malacca, Malaysia. The first step of synthesizing the chitosan from the shrimp shells started with washing the crustaceans with flowing tap water to remove the soil and extraneous matter. The cleaning process is essential to clean the raw shrimp shell material before proceeding to the next step. The pre-treatment steps improved the quality of chitin and chitosan in terms of minimizing chemical usage and preventing bad odors from the samples [11]. The cleaned shrimp shell sample was dried in a hot air oven at 90 °C until a constant weight was achieved. Next, the dried shrimp shell was blended until it was a homogenous-sized powder using a kitchen blender. In this paper, the characterization of chitosan sample processing was divided into three different types of processes which are demineralization, deproteinization and deacetylation. Table 1 shows the details of the three stages used for the four different samples.

Table 1. Summary of demineralization, deproteinization, and deacetylation processes for shrimp shell samples S1, S2, S3, and S4, detailing the specific conditions for each step.

Process	Details
Demineralization	**S1:** 10 g shrimp shell + 80 ml 1 M HCl, Stir 5h, RT, 250 rpm, Soak 16h, Ethanol 20 min, Oven 70°C, 8h **S2:** Same as S1, Soak 17h **S3:** Same as S1, Soak 17h **S4:** Same as S1, Soak 17h
Deproteinization	**S1:** Sample + 1 M NaOH (1:10 g/ml), Stir 3h, 80°C, 250 rpm, No soak, Ethanol 10 min, Oven 70°C, 7-8h **S2:** Same as S1, Stir 1h, Soak 22h, Repeat twice **S3:** Same as S2, Soak 48h **S4:** Stir 1h, 60-70°C, Soak 5 days, Oven 80°C, 10h
Deacetylation	**S1:** Sample + 12.5 M NaOH (1:30 g/ml), Stir 2.5h, 115-120°C, No soak, Oven 70°C, 6h **S2:** Stir 1h, 100-120°C, Soak 24h, Repeat twice **S3:** Same as S1, Soak 2 days, Oven 80°C, 10h **S4:** Stir 2.5h, 70-80°C, Soak 5 days, Oven 80°C, 10h

Demineralization Process

After the pre-treatment of the sample, the process continued with the demineralization process by adding 1 M HCl to the dried sample powder with a 1:10 solid-to-solvent ratio, w/v. The stirring process proceeded at room temperature under agitation at 250 rpm for a few hours. Next, the demineralized shells were filtered using pump filtration and washed with distilled water until they reached neutral pH. It was important to achieve a neutralized sample before the next process proceeded. To further remove impurities from the samples, samples were bleached by immersing in ethanol for a few minutes and then drying in an oven at 70 °C until a constant weight was reached. Figure 1 shows the process of filtration of shrimp shell after HCL was added into the samples.

Fig. 1. Process of filtration of shrimp shell in demineralization process.

Deproteinization

The deprotienization process was undertaken by mixing the dried demineralized powder with 1 M of NaOH solution at a solid/liquid ratio of 1:10 w/v. The reaction was carried out under agitation at different temperatures and soaking times for each of the samples. After the process was completed, the solids were filtrated and washed with distilled water until neutral pH was achieved. Then the samples were immersed in ethanol for further bleaching, and the resulting chitin was dried in an oven at 70 °C. Figure 2 shows the results from deproteinization of shrimp shell.

Deacetylation

Deacetylation continued the processing by treating the chitin with a strong alkaline solution of 12.5 M NaOH at a solid/liquid ratio of 1:15 (g/mL). The process was achieved by using different temperatures and soaking times as shown in the Table 1. The resulting chitosan was filtrated, washed with distilled water until neutral pH was reached and dried in an oven at 70 °C. This resulted in the production of chitosan flakes. The deacetylation treatment produced chitosan which is a soluble polymer in acid aqueous medium. Figure 3 shows the chitosan flakes produced after going through the deacetylation process.

Fig. 2. Results from deproteinization of shrimp shell.

Fig. 3. Chitosan powder prepared from shrimp shell.

RESULTS

Solubility

Chitosan is known to be completely soluble in concentrated acids and partially soluble in dilute acid solutions. Many studies presented the solubility of chitosan in acetic acid at 1-2% [12]. For solubility studies, 3 mg of each of the chitosan samples were dissolved in 3 ml of 1% acetic acid and stirred using a magnetic stirrer until a homogenous solution was obtained as shown in Figure 4. From the observations, all of the samples were completely dissolved in acetic acid. Due to the obvious protonation of amino groups, chitosan is soluble in aqueous acids, but it is insoluble in water and most organic solvents, thus limiting its applications[13]. Chitosan's enhanced solubility is attributed to its structure, which differs significantly from that of chitin. Through deacetylation, chitosan's acetyl groups are partially removed, exposing amine groups ($-NH_2$) that increase hydrophilicity and enable dissolution in dilute acidic conditions. Based on the studies from [14], if the solvent/chitosan ratio was increased, the solubilization time also increased.

Fig.4. Solubility of chitosan (S1-S4) in 1% acetic acid.

FTIR Characterization

The Fourier transform infrared (FTIR) spectra of S1 to S4 in the 400–4000 cm^{-1} range are shown in Figure 5. FTIR studies were conducted for the different methods (temperatures and soaking times) used for the four samples. The absorption peaks at wavenumber 2872.17 cm^{-1} were due to the presence of methylene and methyl groups in the chitosan structure [15]. From the observations of the samples S1-S4, S2 produced a small peak compared with the other samples. From the results observed, all of the samples, S1-S4, produced an absorption at wavenumber 1644.49 cm^{-1} which indicates the C=O stretching vibration. This result is the same absorption as in [15]. Wavenumber 1590.72 cm^{-1} was indicated for all samples, representing the vibration absorption NH_2 groups. Meanwhile, the broad peak at wavenumber 3261 indicated the presence of three different stretching groups, as explained in [16,17]. Samples 3 and 4 showed higher intense peaks which appeared at 1149 cm^{-1} and 1031 cm^{-1}, possibly caused by characteristic peaks of C-N stretching vibration and is evidence of the amine group presence. The peaks were also similar to the peak found in [18]. The decrease in the intensity of the 1650 cm^{-1} (approximately) band corresponds to the carboxyl group and reflects a deacetylation process [19].

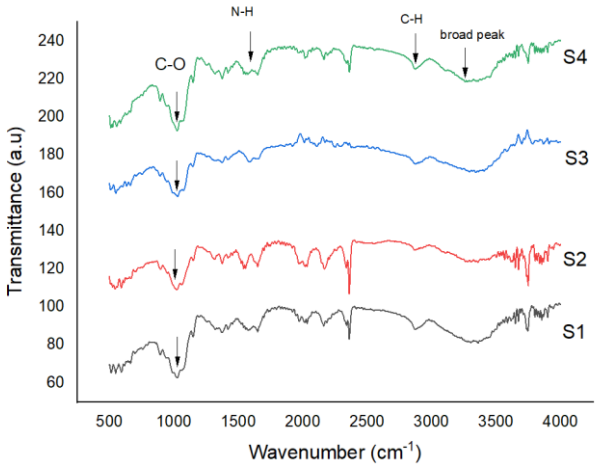

Fig.5. Infrared spectra of chitosan of S1-S4.

The DD is one of the chitosan characterization approaches that is often discussed in the literature. The most precise technique to measure DD is nuclear magnetic resonance (NMR) spectroscopy [20]. However, this technique requires higher costs compared with other techniques. So the research from [20] presented various calculation techniques based on UV-Vis and infrared spectroscopy. There is a range of bands of wavelength that have been chosen to measure the DD [20,21]. In this paper, further examination of chitosan DD used infrared spectroscopy. The DD was determined according to the calculation from [3]. The A1320 and A1420 were the peak areas of 1320 cm^{-1} and 1420 cm^{-1}, respectively. The peak at 1320 cm^{-1} is the amide group's distinctive band. DD can be calculated using the formula in Equation 1 as follows [3].

$$\% \text{ DA} = \frac{\left(\frac{A1320}{A1420}\right) - 0.3822}{0.03133} \qquad \textbf{Eq. 1.}$$

%DDA = 100 - %DA
Where, DDA = degree of deacetylation (%),
DA= degree of acetylation (%)

Table 2 represents DD% values of S1 to S4. From the results, S1 has the lowest DD% compared with the others. DD% in this paper was also found to be similar to [22]. During the deproteinization and deacetylation processes, S1 was not involved in any soaking treatment with chemicals after the stirring process. The highest DD% was obtained from S4. The results showed an increase in DD% when using longer soaking times during the deproteinization and deacetylation processes and higher temperatures produced a higher DD% (80.4818) compared to lower soaking times [7,11]. According to [3], DD% was increased when the deacetylation process was repeated twice with the aid of heating elements. In addition, all the samples that were soaked in HCl solution showed the total bacterial count of treated samples to be decreased [11].

There were three ranges of DD% that were discussed in [23] whereby the range of 55-70% of DD was classified as a low deacetylated degree of chitosan, which was entirely insoluble in water. A deacetylation degree of 70-85% was classified as the middle deacetylation degree of chitosan. In this paper, the chitosan was in the area of ~80% which may be partly dissolved in water. Finally, the range of 85-95% accomplished a good solubility in water and it is known as very high DD of chitosan, which is difficult to achieve. As DD rises, the chitosan backbone gains more amino groups, increasing the hydrophilicity of the chitosan films, and thus S1 (Sample1) increases correspondingly [13], because the higher the DD, the more amino groups there are in the molecule. The protonation of the -NH_2 functional group is vital for chitosan's biological effects and water solubility to show up [8].

Table 2. Calculation of DD% for different types of samples.

Sample / Peak Area	A1320	A1420	DD%
S1	88.1958	88.1508	80.264
S2	89.8743	90.2305	80.406
S3	92.0779	92.6352	80.472
S4	84.9688	85.5073	80.481

XRD Characterization

The crystalline structures of chitosan were determined by powder X-ray diffraction (XRD). The patterns indicate a crystallized structure at 2θ = 20°, which is the most intense peak height for the chitosan sample. This peak occurred in polymorphic forms in shrimp and crab shells [24], from the XRD result as shown in Figure 6. S1 and S3 produced higher intensity at 020 compared with other samples. It is shown that with decreasing DD values, the intensity at 020 is higher [13,24]. A small peak was observed near 2θ = 30° for S1, which was discussed as the formation of calcite and calcium phosphate family interferences [25]. The broad peak observed at both 020 and 110 was similar to [26].

From the results observed, the intensity at 020 reflections decreased when the DD was increased and moved the second peak at 110 reflections, and is also decreased when higher DD% was produced (S4: 80.48 %). This linear relationship between CrI020 and DD suggested that XRD determines the DD of macromolecular chitin and chitosan [24]. From the samples soaked in HCl had lower DD values than unsoaked samples. This might be caused by the long-term degradation of chitin and chitosan during the soaking step in the HCl solution. Trung et al. also observed low degradation of chitin and chitosan caused by the longer soaking time [11]. These samples are classified as chitosan based on an 80% degree of deacetylation (DDA). Chitosan is derived from chitin through deacetylation, where some of the acetyl groups are removed to expose amine groups (–NH_2) on the polymer chain. This alteration increases the hydrophilicity of chitosan. Chitosan has a more flexible structure compared to chitin due to the presence of these free amine groups, which can interact with water molecules, enabling it to dissolve in acidic solutions (e.g., dilute acetic acid).

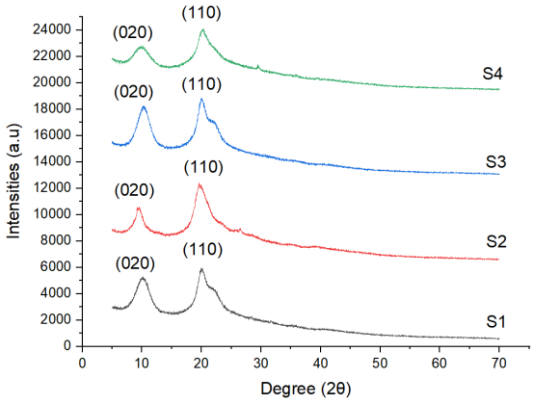

Fig.6. XRD patterns of chitosan films with various degrees of crystallinity.

UV-Vis Characterization

In the UV-Vis spectroscopy process, electromagnetic radiation within the wavelength range of 200–1100 nm is absorbed and electrons are then excited to higher energy states. The fabrication into chitosan film was started by dissolving the samples (S1-S4) in 1% acetic acid at room temperature under constant stirring. Then the chitosan solutions were obtained by spin coating the film onto a 2x2 cm glass slide at the same speed. Figure 7 shows the characteristic chitosan absorption below 300 nm, revealing the presence of chitosan. There was no discernible difference between the four samples (S1-S4), and the spectra showed very weak absorptions at wavelengths of more than 300 nm.

The wavelength versus absorption curve was plotted, and the optical band gap energy value was determined using Tauch plot methods. Tauch plotting is a technique for determining the optical band gap by examining the linear relationship graph. The relation between photon energy (hv) and absorption coefficient (α) was determined by [27]as in Equation 2 below:

$$(\alpha hv)\frac{1}{n} = k(hv - Eg) \qquad \textbf{Eq.2}$$

Where hv is the photon energy, h is Plank's constant, Eg is the optical band gap, k is constant and n is the transition state, i.e., direct or indirect transitions. A direct transition occurs when a photon excites an electron directly from the valence band to the conduction band if the momentum of electrons and holes in both bands is identical (conduction and valence). For direct transition, n = 1/2 is substituted in Equation 2. Figure 8 shows the determination of the optical gap series for all thin-film chitosan samples obtained by the straight-line intersection. The calculated values of bandgap were 4.06 eV for Sample 1, 4.04 eV for Sample 2, 4.02 eV for Sample 3, and 4.06 eV for Sample 4. The results attained were higher than the 2 eV which was reported from [28,29]. This could be due to the different thicknesses and sample preparations of chitosan concentration.

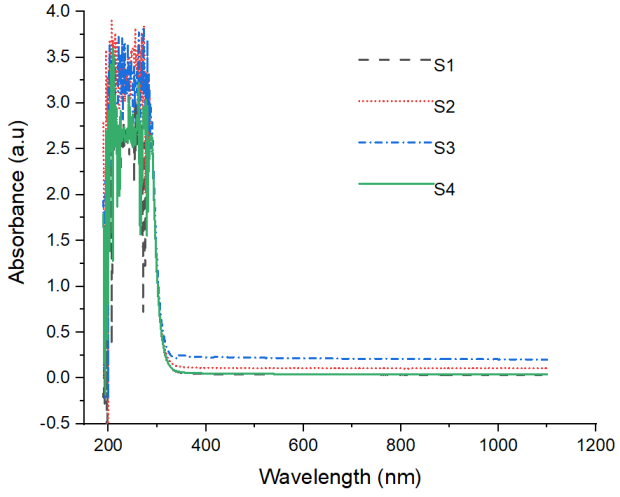

Fig.7. UV-Vis absorption spectra for different samples of chitosan (S1-S4).

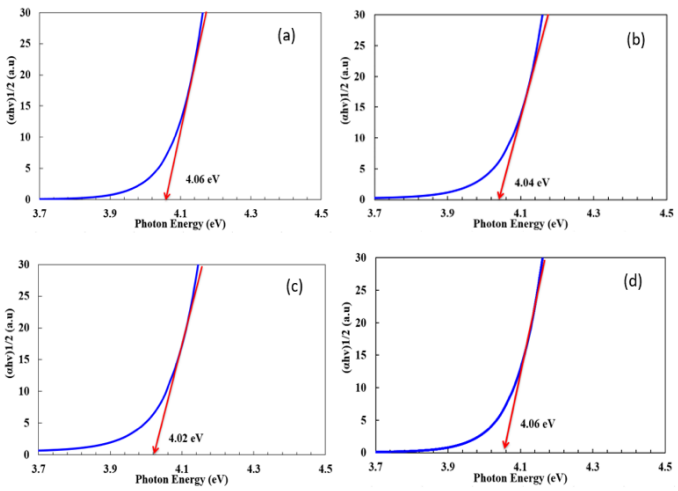

Fig.8. The determination of the optical gap energies of chitosan sample (a) S1, (b) S2, (c) S3, (d) S4

CONCLUSION

The extracted chitosan from shrimp shells was characterized by FTIR, XRD, and UV-Vis techniques. Four methods were used to synthesize chitosan, involving variations in soaking times and temperatures. The FTIR results showed varying degrees of deacetylation (DD%) across the samples, with an observed increase in DD% as the soaking time during demineralization, deproteinization, and deacetylation processes was extended. Sample 4 exhibited the highest DD% along with a less crystalline structure, as determined by XRD analysis. All chitosan samples were fully soluble in acetic acid, indicating high purity. The XRD patterns indicated an amorphous structure for all samples, suggesting that the chitosan can act as a polymer, with sharper peaks signifying greater crystallinity. The crystallinity of the chitosan appeared to decrease with increasing DD%, with Sample 4 (80.48% DDA) displaying the lowest crystallinity.

Peer-review: Externally peer-reviewed.

Author Contributions: Concept – S.A.C.A; Design – S.A.C.A; Supervision – S.A.M.C, N.H.S.; Resources – S.A.C.A.; Data Collection and/or Processing – S.A.C.A.; Analysis and/or Interpretation – S.A.C.A.; Literature Search – S.A.C.A.; Writing Manuscript – S.A.C.A.; Critical Review – S.A.M.C, N.H.S.

Conflict of Interest: The authors have no conflicts of interest to declare.

Financial Disclosure: The authors declared that this study has received no financial support

REFERENCES

1. Pambudi GBR, Ulfin I, Harmami H, Suprapto S, Kurniawan F, Ni'mah YL. Synthesis of water-soluble chitosan from crab shells (Scylla serrata) waste. In: *AIP Conference Proceedings*. Vol 2049. AIP Publishing; 2018:020086. doi:10.1063/1.5082491

2. Chakravarty J, Yang C-L, Palmer J, Brigham CJ. Chitin extraction from lobster shell waste using microbial culture-based methods. *Appl food Biotechnol*. 2018;5(3):141-154. doi:10.22037/afb.v5i3.19628

3. Ahing FA, Wid N. Optimization of shrimp shell waste deacetylation for chitosan production. *Int J Adv Appl Sci*. 2016;3(10):31-36. doi:10.21833/ijaas.2016.10.006

4. Huang Y-L, Tsai Y-H. Extraction of chitosan from squid pen waste by high hydrostatic pressure: Effects on physicochemical properties and antioxidant activities of chitosan. *Int J Biol Macromol*. 2020;160:677-687. doi:10.1016/j.ijbiomac.2020.05.252

5. Charoenvuttitham P, Shi J, Mittal GS. Chitin Extraction from Black Tiger Shrimp (Penaeus monodon) Waste using Organic Acids. *Sep Sci Technol*. 2006;41(6):1135-1153. doi:10.1080/01496390600633725

6. Benhabiles MS, Salah R, Lounici H, Drouiche N, Goosen MFA, Mameri N. Antibacterial activity of chitin, chitosan and its oligomers prepared from shrimp shell waste. *Food Hydrocoll*. 2012;29(1):48-56. doi:10.1016/j.foodhyd.2012.02.013

7. Younes I, Rinaudo M. Chitin and Chitosan Preparation from Marine Sources. Structure, Properties and Applications. *Mar Drugs*. 2015;13(3):1133-1174. doi:10.3390/md13031133

8. Kou S (Gabriel), Peters LM, Mucalo MR. Chitosan: A review of sources and preparation methods. *Int J Biol Macromol*. 2021;169:85-94. doi:10.1016/j.ijbiomac.2020.12.005

9. Suryawanshi N, Jujjavarapu SE, Ayothiraman S. Marine shell industrial wastes–an abundant source of chitin and its derivatives: constituents, pretreatment, fermentation, and pleiotropic applications-a revisit. *Int J Environ Sci Technol*. 2019;16(7):3877-3898. doi:10.1007/s13762-018-02204-3

10. Percot A, Viton C, Domard A. Optimization of Chitin Extraction from Shrimp Shells. *Biomacromolecules*. 2003;4(1):12-18. doi:10.1021/bm025602k

11. Trung TS, Tram LH, Van Tan N, et al. Improved method for production of chitin and chitosan from shrimp shells. *Carbohydr Res*. 2020;489:107913. doi:10.1016/j.carres.2020.107913

12. Saisa, Agusnar H, Alfian Z, Nainggolan I. The effect of Acetic Acid Ratio in The Electrodeposition Process of Chitosan/ZnO. *J Phys Conf Ser*. 2019;1232(1):012011. doi:10.1088/1742-6596/1232/1/012011

13. Feng F, Liu Y, Zhao B, Hu K. Characterization of half N-acetylated chitosan powders and films. *Procedia Eng*. 2012;27:718-732. doi:10.1016/j.proeng.2011.12.511

14. Khanafari A, Marandi R, Sanati SH. Recovery of chitin and chitosan from shrimp waste by chemical and microbial methods. *Iran J Environ Heal Sci Eng*. 2008;5(2):19-24. https://www.sid.ir/en/VEWSSID/J_pdf/102620080104.pdf

15. Rochima E, Azhary SY, Pratama RI, Panatarani C, Joni IM. Preparation and Characterization of Nano Chitosan from Crab Shell Waste by Beads-milling Method. *IOP Conf Ser Mater Sci Eng*. 2017;193:012043. doi:10.1088/1757-899X/193/1/012043

16. Cadogan EI, Lee C-H, Popuri SR, Lin H-Y. Effect of Solvent on Physico-Chemical Properties and Antibacterial Activity of Chitosan Membranes. *Int J Polym Mater Polym Biomater*. 2014;63(14):708-715. doi:10.1080/00914037.2013.867264

17. Kumirska J, Czerwicka M, Kaczyński Z, et al. Application of Spectroscopic Methods for Structural Analysis of Chitin and Chitosan. *Mar Drugs*. 2010;8(5):1567-1636. doi:10.3390/md8051567

18. Yuan W, Yin XQ, Tu WP, Lin Q, Cao Y. Chitosan Pyruvic Acid Derivatives: Preparation, Moisture Absorption-Retention Ability and Antioxidative Activity. *Key Eng Mater*. 2007;361-363:963-966. doi:10.4028/www.scientific.net/KEM.361-363.963

19. Borja-Urzola A del C, García-Gómez RS, Flores R, Durán-Domínguez-de-Bazúa M del C. Chitosan from shrimp residues with a saturated solution of calcium chloride in methanol and water. *Carbohydr Res*. 2020;497:108116. doi:10.1016/j.carres.2020.108116

20. Czechowska-Biskup R, Jarosińska D, Rokita B, Ulański P, Rosiak JM. Determination of degree of deacetylation of chitosan-comparision of methods. *Prog Chem Appl Chitin its Deriv*. 2012;(17):5-20.

21. Brugnerotto J, Lizardi J, Goycoolea F., Argüelles-Monal W, Desbrières J, Rinaudo M. An infrared investigation in relation with chitin and chitosan characterization. *Polymer (Guildf)*. 2001;42(8):3569-3580. doi:10.1016/S0032-3861(00)00713-8

22. Eddya M, Tbib B, EL-Hami K. A comparison of chitosan properties after extraction from shrimp shells by diluted and concentrated acids. *Heliyon*. 2020;6(2):e03486. doi:10.1016/j.heliyon.2020.e03486

23. Lv SH. High-performance superplasticizer based on chitosan. In: *Biopolymers and Biotech Admixtures for Eco-Efficient Construction Materials*. Elsevier; 2016:131-150. doi:10.1016/B978-0-08-100214-8.00007-5

24. Zhang Y, Xue C, Xue Y, Gao R, Zhang X. Determination of the degree of deacetylation of chitin and chitosan by X-ray powder diffraction. *Carbohydr Res*. 2005;340(11):1914-1917. doi:10.1016/j.carres.2005.05.005

25. Sawada M, Sridhar K, Kanda Y, Yamanaka S. Pure hydroxyapatite synthesis originating from amorphous calcium carbonate. *Sci Rep*. 2021;11(1):11546. doi:10.1038/s41598-021-91064-y

26. De Queiroz Antonino R, Lia Fook B, De Oliveira Lima V, et al. Preparation and Characterization of Chitosan Obtained from Shells of Shrimp (Litopenaeus vannamei Boone). *Mar Drugs*. 2017;15(5):141. doi:10.3390/md15050141

27. Fauzi NIM, Fen YW, Omar NAS, et al. Nanostructured Chitosan/Maghemite Composites Thin Film for Potential Optical Detection of Mercury Ion by Surface Plasmon Resonance Investigation. *Polymers (Basel)*. 2020;12(7):1497. doi:10.3390/polym12071497

28. Balyan M, Nasution TI, Nainggolan I, Mohamad H, Ahmad ZA. Effect Band Gap of Chitosan Film in Converting Water Vapour Into Electrical Current. *Mater Sci Forum*. 2020;1010:445-452.

doi:10.4028/www.scientific.net/MSF.1010.445

29. Abdi MM, Ekramul Mahmud HNM, Abdullah LC, Kassim A, Zaki Ab. Rahman M, Chyi JLY. Optical band gap and conductivity measurements of polypyrrole-chitosan composite thin films. *Chinese J Polym Sci*. 2012;30(1):93-100. doi:10.1007/s10118-012-1093-7